Cytochrome P-450 Catalyzed Insecticide Metabolism. Prediction of Regio- and Stereoselectivity in the Primer Metabolism of Carbofuran: A Theoretical Study

György M. Keserü,*,†,‡ István Kolossváry,*,‡,§ and Béla Bertók†

Contribution from the Department of Chemical Research, CHINOIN AGCHEM Business Unit, P.O. Box 49, H-1780, Budapest, Hungary, and Department of Chemical Information Technology, Technical University of Budapest, Szt. Gellért tér 4, H-1111, Budapest, Hungary

Received November 13, 1996. Revised Manuscript Received March 21, 1997[⊗]

Abstract: The molecular mechanism of carbofuran metabolism was investigated by molecular modeling using the energy-minimized active site of cytochrome P-450$_{cam}$. A feasible binding conformation of carbofuran was subjected to Monte Carlo (MC) conformational search and molecular dynamics (MD) simulation in the active site to obtain the global minimum of the enzyme−substrate complex. For exploring its conformational space, MC was found to be more effective than simple MD. Enzyme−substrate interactions were examined in detail in all low-energy states. Distances between the active ferryl oxygen of the central heme unit and the reactive centers of carbofuran involved in oxidative metabolism were monitored. H-bonding interaction between the carbamate group of carbofuran and the Tyr96-OH group, as well as the steric effects of Val247 and Val295, were found to be crucial for the orientation of carbofuran. The preferred formation of 3-hydroxycarbofuran, the major primer metabolite, could be rationalized by the model. The configuration at the C3 atom was predicted to be *S* in accordance with the stereospecificity reported for the natural substrate.

Introduction

Microsomal cytochrome P-450 dependent monooxygenases are recognized as key factors in insecticide metabolism.[1] In addition to the regulation of endogenous compounds, their role in the detoxication of xenobiotics (e.g., drugs, pesticides, and plant toxins) is characteristic. P-450 monooxygenases can be classified into two important families: cytochrome P-450 and NADPH−cytochrome P-450 reductase, which are typically found in the endoplasmaic reticulum of almost all eukaryotes, such as plants, fungi, insects, and vertebrates. Multifunctional activity of insect P-450 monooxygenases[2] involves the influence on growth, development, and feeding, as well as development of resistance against pesticides and tolerance of plant toxins.[3] Recent efforts on the integrated management of resistance were initiated by the increasing doses of pesticides on formerly susceptible strains of pests.

Polysubstrate monooxygenases participate in at least four metabolic reactions such as hydroxylation (aliphatic and aromatic), dealkylation (O- and N-dealkylation), epoxidation, and sulfoxidation.[4] Research on these metabolic pathways has shed some light on the possible target points, where metabolic activities and insect resistance could be reduced.[5,6]

The role of cytochrome P-450 in insecticide resistance was first substantiated by Eldefrawi et al. abolishing carbaryl resistance with the (methylenedioxy)phenyl synergist Sesamex.[7] P-450 monooxygenase mediated detoxication has further been supported by experimental evidence[8,9] and identified as one of the most important mechanisms of resistance in a large number of pests.[10−12] Similar to carbaryl and other systemic insecticides, resistance to carbofuran (**1**) has been linked to an increased rate of metabolism. Resistant strains of houseflies and Colorado beetles against **1** were originally raised by Rose and Brindley.[13] This resistance could be almost eliminated by simultaneous application of piperonyl butoxide (PBO) and **1**. The considerable decrease of corresponding LD_{50} values indicates that monooxygenases are likely to play an important role in the mechanisms of carbofuran resistance,[14] which prompted us to investigate the cytochrome P-450 assisted metabolism of **1** on a molecular basis.

Oxidative metabolism of **1** has extensively been studied in plants, insects, and mammals.[15−19] On the basis of radiolabeled studies,[20] the major metabolite was identified as 3-hydroxycar-

† CHINOIN AGCHEM Business Unit.
‡ Technical University of Budapest.
§ Present address: Department of Chemistry, Columbia University, New York, New York 10027.

⊗ Abstract published in *Advance ACS Abstracts,* May 15, 1997.

(1) Ortiz de Montellano, P. R., Ed. *Cytochrome P-450*; Plenum Press: New York, 1995.
(2) Romis, M. J.; Hodgson, E. *Xenobiotica* **1989**, *19*, 1077−1092.
(3) Agosin, M. In *Comprehensive Insect Physiology, Biochemistry and Pharmacology*; Kerkut, G. A.; Gilbert, L. I., Eds.; Pergamon Press: Oxford, 1985; Vol. 12, p 647.
(4) Kulkarni, A.; Hodgson, E. *Annu. Rev. Pharmacol. Toxicol.* **1984**, *24*, 19−42.
(5) Mulin, C. A.; Scott, J. G., Eds. *Molecular Mechanism of Insecticide Resistance*; ACS Symposium Series No. 505; American Chemical Society: Washington, DC, 1992.
(6) Hodgson, E.; Rose, R. L.; Goh, D. K.; Rock, G. C.; Roe, R. M. *Biochem. Soc. Trans.* **1993**, *21*, 1060−1065.
(7) Eldefrawi, M. E.; Miskus, R.; Sutcher, V. *J. Econ. Entomol.* **1960**, *53*, 231−234.
(8) Georghiou, G. P.; Metcalf, R. L.; March, R. B. *J. Econ. Entomol.* **1961**, *54*, 132-135.
(9) Schonbrod, R. D.; Philleo, W. W.; Terriere, L. C. *J. Econ. Entomol.* **1965**, *58*, 74-77.
(10) Wilkinson, C. F. In *Pest Resistance to Pesticides*; Georghiou, G. P., Saito, T., Eds.; Plenum Press: New York, 1983; p 175.
(11) Ishaaya, I. *Arch. Insect Biochem. Physiol.* **1993**, *22*, 263−276.
(12) Feyereisen, R. *Toxicol. Lett.* **1995**, *82/83*, 83−90.
(13) Rose, R. L.; Brindley, W. A. *Pestic. Biochem. Physiol.* **1985**, *23*, 74−81.
(14) Hassal, K. A. *The Biochemistry and Uses of Pesticides*; VCH: Weinheim, 1990; p 124.
(15) Knaak, J. B.; Munger, D. M.; McCarthy, J. *J. Agric. Food Chem.* **1970**, *18*, 827-839.
(16) Ashworth, R. J.; Sheets, T. J. *J. Agric. Food Chem.* **1972**, *20*, 407−412.
(17) Pree, D. J.; Saunders, J. L. *J. Agric. Food Chem.* **1974**, *22*, 620−625.
(18) Marshall, T. C.; Dorough, H. W. *J. Agric. Food Chem.* **1977**, *25*, 1003−1009.

S0002-7863(96)03937-6 CCC: $14.00

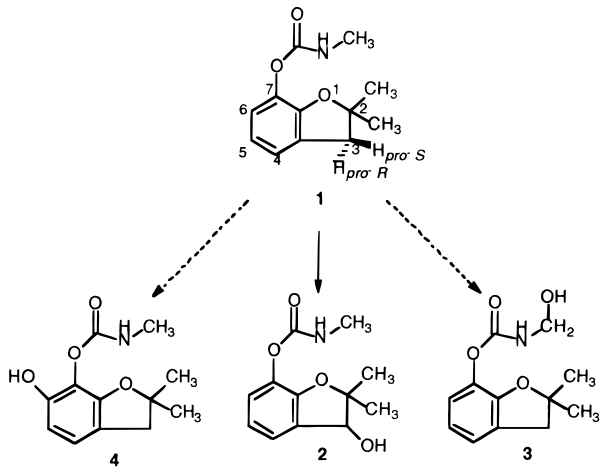

Figure 1. Primer oxidative metabolism of carbofuran in insects.

bofuran (**2**), along with the corresponding *N*-methyl-hydroxylated product **3** as a minor component (Figure 1). Hydrolysis of the ester linkage of primary metabolites as well as conjugation reactions has also been detected.

Here we report our investigation on the metabolism of **1** in order to rationalize the formation of its primary metabolites.

Methods

All computations were carried out on a Silicon Graphics Indy workstation using the MacroModel 4.5[21] and SPARTAN 3.1[22] program packages for biomolecules and organic intermediates, respectively.

Conformational Analysis of Carbofuran (1). Due to the condensed structure of **1**, only three torsional degrees of freedom were identified at the aliphatic carbamate side chain. Conformational analysis was performed by the systematic variation of all three torsional angles using the Tripos force field[23] and electrostatically fitted charges obtained by AM1 semiempirical calculations[24] using SPARTAN 3.1.

Relative Stability of Possible Radical Intermediates. Relative stabilities of radicals that could be formed by hydrogen abstraction from the carbon atom at the 3-position and from the carbon atom connected to the carbamate nitrogen were calculated. Geometry optimization of radicals was started from the lowest energy conformation of carbofuran using AM1-UHF calculations in SPARTAN 3.1. Ionization potentials were approximated according to Koopman's theorem,[25] as the negative of the energy of the highest singly-occupied molecular orbital.

Enzyme−Substrate Interactions. Enzyme−substrate interactions are best studied if a three-dimensional structure of the corresponding metabolic enzyme is available. Lacking the structural information of the specific enzyme, we used the crystal structure of adamantanone-bound cytochrome P-450$_{cam}$[26] to predict the interactions of **1**. A binding site model was defined as an approximately 12 Å sphere around the central heme unit. This model is composed of 87 amino acids, 7 bound water molecules, and the protoporphyrin IX heme unit including the putative, biologically active ferryloxy species. The ferryloxy model was constructed by placing an oxygen atom perpendicular to the porphyrin plane opposite from the cysteinate ligand at a distance of 1.7 Å, which is consistent with the value obtained from XAFS[27] and ENDOR[28] studies.

Table 1. AMBER* Parameters for the Ferryloxy Heme Unit and **1**

stretching param	force constant (kcal/Å^2)	r_0 (Å)	stretching param	force constant (kcal/Å^2)	r_0 (Å)
Fe−S	200	2.20	Fe−O	200	1.70
bending param	**force constant (kcal/Å^2)**	**θ_0 (deg)**	**bending param**	**force constant (kcal/Å^2)**	**θ_0 (deg)**
C_β−S−Fe	150	109.0	N−Fe−O	50	90.0
S−Fe−N	40	98.0	S−Fe−O	10	180.0
nonbonded param	**constant (kcal/mol)**	**r_0 (Å)**	**nonbonded param**	**constant (kcal/mol)**	**r_0 (Å)**
S_{fer}	0.20	2.00	Fe	0.20	0.95
O_{fer}	0.15	1.65			

Table 2. Electrostatic Atomic Charges for the Ferryloxy Heme Unit and **1** Obtained by STO-3G and AM1 Calculations, Respectively

atom	charge	atom	charge
C1	−0.38	*C*=O	0.99
C2	0.31	C=*O*	−0.55
C3	−0.09	*N*CH$_3$	−0.75
C3a	−0.09	NC*H*$_3$	0.24
C4	−0.10	Fe	1.53
C5	−0.17	S	−0.65
C6	−0.10	C_β	−0.12
C7	0.20	C_{heme}	0.15
C7a	0.14	O_{fer}	−0.67
2-CH$_3$	−0.24	C_{prop}	0.34
7-O	−0.46	N_{pyr}	−0.41

Docking calculations were performed using the united-atom representation of the AMBER* force field[29] available in MacroModel. Parameters and atomic charges for the ferryloxy heme unit as well as for carbofuran are shown in Tables 1[30] and 2, respectively. The complexed adamantanone was substituted by the minimum-energy conformation of carbofuran, and a constrained energy minimization was performed using the Polaak−Ribiere conjugate gradient method with the convergence criterion set to 0.01 kJ/(Å mol). Construction of the binding site model afforded that the 87 amino acids were not contiguous in the protein and therefore all the backbone atoms had to be constrained. Constraints (35 kJ/Å^2) were introduced by a harmonic restoring potential, while all side chains, porphyrin, and the substrate were free to move. The electrostatic treatment of the enzyme−substrate complex involved a distance-dependent dielectric constant ($\epsilon = 1.0$) as a simple model for the screening of charge−charge interactions by the solvent. Cutoff distances were extended to 8 Å for van der Waals and 20 Å for charge−charge interactions considering long-range electrostatic interactions in the protein environment.

Conformational search of the enzyme-bound **1** was performed by the Monte Carlo method[31] for the random variation of all of the rotatable bonds combined with the so-called variable molecules selection (MacroModel MOLS option) for translations and rotations of the ligand in the binding site. The MOLS command allows a selected molecule or molecules to move during a Monte Carlo (MC) step by randomly selected rotations and/or translations with respect to a fixed active site and, therefore, is particularly useful for docking calculations. Translations and rotations within the binding site in combination with a 1000

(19) Marshall, T. C.; Dorough, H. W. *Pestic. Biochem. Physiol.* **1979**, *11*, 56−59.
(20) Metcalf, R. L.; Fukuto, T. R.; Collins, C.; Borck, K.; El-Aziz, S. A.; Munoz, R.; Casida, C. C. *J. Agric. Food Chem.* **1968**, *16*, 300−311.
(21) MacroModel V4.5, Department of Chemistry, Columbia University, New York , NY 10027, 1994.
(22) SPARTAN V3.1, Wavefunction Inc., 18401 Von Karman Ave., #370, Irvine, CA 92715, 1994.
(23) Clark, M.; Cramer, R. D., III; Van Opdenbosch, N. *J. Comput. Chem.* **1989**, *10*, 982−1012.
(24) Dewar, M. J. S.; Zoebisch, E. G.; Healy, E. F.; Stewart, J. J. P. *J. Am. Chem. Soc.* **1985**, *107*, 3902−3909.
(25) Koopman, T. *Physica* **1933**, *1*, 104.
(26) Raag, R.; Poulos, T. *Biochemistry* **1991**, *30*, 2674−2684.
(27) Chance, B.; Powers, L.; Ching, Y.; Poulos, T.; Schonbaum, G. R.; Yamazaki, G. R.; Paul, K. G. *Arch. Biochem. Biophys.* **1984**, *235*, 596−611.
(28) Goldfarb, D.; Bernardo, M.; Thomann, H.; Kroneck, P. M. H.; Ulbrich, V. *J. Am. Chem. Soc.* **1996**, *118*, 2686−2693.
(29) Singh, U. C.; Weiner, P. K.; Caldwell, J. W.; Kollman, P. A. AMBER UCSF V3.0a, Department of Pharmaceutical Chemistry University of California at San Francisco, 1986.
(30) Collins, J. R.; Camper, D. L.; Loew, G. H. *J. Am. Chem. Soc.* **1991**, *113*, 2736−2743.
(31) Chang, G.; Guida, W. C.; Still, W. C. *J. Am. Chem. Soc.* **1989**, *111*, 4379−4386.

Table 3. Distribution of Low-Energy Conformers of **1** at 300 K, Obtained by a Grid Search

conformer	energy (kcal/mol)	Boltzmann population (%)	conformer	energy (kcal/mol)	Boltzmann population (%)
1	17.974	54.6	4	19.436	4.6
2	18.351	18.9	5	20.547	0.7
3	18.925	10.9	6	21.255	0.2

step MC conformational search of the substrate enabled us to look for all possible binding geometries.

The usefulness of this approach was demonstrated in a comparative molecular dynamics (MD) simulation of **1** in the same binding model. Constant temperature MD was performed at 300 K using the SHAKE algorithm[32] and the electrostatic treatment described previously. The same manually docked starting structure was subjected to 2000 steps of Polaak−Ribiere conjugate gradient minimization. The resulting structure was then equilibrated for 30 ps before the accumulation of a 150 ps long dynamics data analysis. A total of 1000 structures were sampled periodically along equilibrated dynamic trajectories. These structures were finally subjected to energy minimization to yield 68 unique binding conformations. The global minimum was found to be closely related to that obtained by MCMM/MOLS (RMS for the non-hydrogen atoms of the substrate, 0.106 Å).

Results and Discussion

Conformational Analysis of Carbofuran. Due to the relatively few degrees of rotational freedom in **1**, the conformational space was explored by the straightforward grid search technique, where the torsional step size of 10° was applied. The low-energy conformers were identified by setting the minimum Boltzmann population cutoff to 0.1 (Table 3).

Relative Stability of Potential Radical Intermediates. Metabolic studies on **1** in insects have demonstrated two possible sites for oxidative metabolism,[20] hydroxylation at the 3 position which leads to the major metabolite **2**, while hydroxylation at the carbon atom of the *N*-methyl group resulted in the formation of C^N-hydroxycarbofuran (**3**) as a minor metabolite. Traces of 6-hydroxycarbofuran (**4**) corresponding to the hydroxylation of the aromatic carbon atom at position 6 have also been isolated in some cases.

According to the mechanistic proposal of Loew *et al.*,[30] on the basis of both experimental and theoretical evidence, P-450 catalyzed aliphatic hydroxylation takes place via a two-step radical mechanism beginning with hydrogen abstraction from the substrate to form a radical intermediate that rapidly reacts with an OH radical to give rise to the hydroxylated product (Figure 2). Aromatic hydroxylation, however, involves the formation of an intermediate epoxide, whose oxirane ring is opened to yield the corresponding hydroxylated product.[33] Due to the different mechanisms involved in the formation of metabolites **2**, **3**, and **4**, relative stabilities of radical intermediates leading to **2** and **3** can only be compared directly to obtain information on the origin of the preferred formation of the 3-hydroxy metabolite. Heats of formation were calculated to be −61.67 and −61.37 kcal/mol for intermediate radical cations leading to **2** and **3**, respectively. Higher stability of the radical corresponding to metabolite **2** is in accordance with its preferred formation. The difference (0.3 kcal/mol) between the calculated heats of formation, however, is smaller than expected on the basis of experimental metabolic studies and is close to the error limit of these calculations.

Calculation of the ionization potential (IP) of the corresponding radical intermediates might serve as an additional descriptor for the site selection. As postulated earlier,[30,34] formation of the radical intermediate should be followed by an electron donation to the heme unit, and therefore, comparison of ionization potentials may help to identify the preferred path of hydroxylation. IP values (−8.4662 and −8.4018 eV for intermediate radical cations leading to **2** and **3**, respectively) show only a slight difference between the electron-donating features of the radical intermediates; the lower value for **2**, however, is consistent with the product distribution observed in the fairly selective metabolism of **1**.

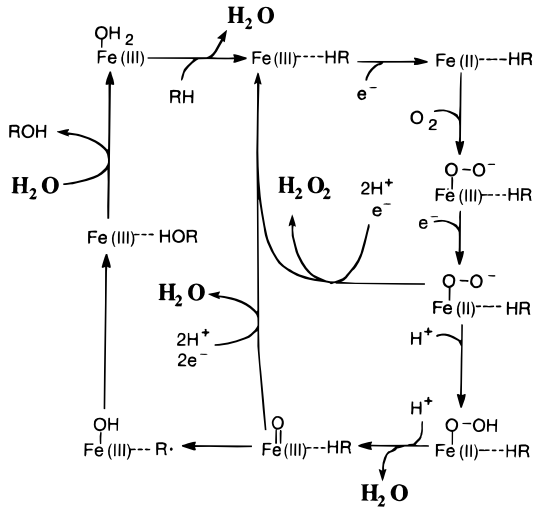

Figure 2. Proposed mechanism of the cytochrome P-450 catalyzed oxidation.

Enzyme−Substrate Interactions. Although the selectivity observed in the primer metabolism of **1** is in accordance with differential electronic properties of the isolated radical intermediates, this model was limited to metabolites formed via chemically similar radical intermediates. Therefore, one can conclude that, considering only the electronic effects, experimental selectivity could not be rationalized. This discrepancy, as well as the small differences between the heats of formation and the ionization potentials of **2** and **3**, urged the application of a more general model. We therefore concluded that the protein environment itself should also be incorporated to reflect our intuition; i.e., the product specificity originates basically from the favored interactions between the substrate and the active site of the enzyme.

Since the three-dimensional structure of the specific P-450 insect protein is unknown, we used the high-resolution structure of cytochrome P-450_{cam}, a bacterial class I monooxygenase. In addition to the stereo- and regioselective hydroxylation of its natural substrate, this enzyme was extensively used as a model for several microsomal oxidations affected by other monooxygenases. Cytochrome P-450_{cam} catalyzed hydroxylation of valproic acid[30] and oxidation of thioanisole to the corresponding sulfoxide,[35] as well as epoxidation of styrene,[36] were carried out successfully. On the basis of reactivity of the cytochrome

(32) Ryckaert, J. P.; Ciccotti, G.; Berendsen, H. J. C. *J. Comput. Phys.* **1977**, *23*, 327−334.
(33) Jerina, D. M.; Daly, J. W. *Science* **1974**, *185*, 573−582.
(34) Harris, D. L.; Loew, G. H. *J. Am. Chem. Soc.* **1994**, *116*, 11671−11674; **1996**, *118*, 6377−6387.
(35) Fruetel, J.; Chang, Y. T.; Collins, J.; Loew, G.; Ortiz de Montellano, P. R. *J. Am. Chem. Soc.* **1994**, *116*, 11643−11648.

P-450$_{cam}$ against the wide range of substrates, it can be concluded that the enzyme active site has not been specifically tailored for a single xenobiotic. A recent review on the structural similarity and functional differences, based on the comparison of the crystal structures of all known P-450s, also concluded that the binding sites of cytochrome P-450$_{cam}$ and P-450$_{terp}$ (terpene monooxygenase) could be similar. Both enzymes hydroxylate small substrates, and the residues critical for substrate access and binding are likely to be located close to, or in, the heme pocket.[37] Observed structural similarity of enzymes incorporating small substrates and the diversity of the potential substrates for P-450$_{cam}$ suggest that this enzyme can serve as a model for the primer oxidative metabolism of **1**.

Enzyme−substrate interactions were studied using the energy-minimized structure of the corresponding macromolecular complex. The initial geometry of the complex was obtained by manual docking of the energetically most favored conformer of **1** to the binding site model of the enzyme constructed as described in the Methods. Minimum energy structures were calculated using the MC conformational search combined with the MOLS routine available in MacroModel.

The MOLS routine allows automatic docking of a ligand in a binding site by a combined conformational search procedure based on variation of the internal degrees of freedom of the ligand (rotatable bonds) as well as the external degrees of freedom of the ligand (relative rotations and translations with respect to the fixed active site).

The internal degrees of freedom of **1** were varied using the MCMM (Monte Carlo multiple minimum) conformational search option[31] of MacroModel which is a highly effective search procedure based on the random torsional variation of the rotatable bonds of the ligand. The combined MCMM/MOLS procedure was applied to allow the simultaneous random translation and rotation of **1** with respect to the active site with increments of 0.5−1.0 Å for the translation of the center of mass of the ligand along the *x*, *y*, and *z* axes and 30−180° for the rotation of the whole ligand around the *x*, *y*, and *z* axes, respectively.

The initial random structures of the complex generated by the combined MCMM/MOLS procedure were subjected to restrained energy minimization by applying a quadratic restoring potential to the backbone atoms of the active site using the FXAT command of MacroModel. FXAT was used with a 35 kJ/A^2 force constant to keep the backbone atoms in place with respect to their location in the crystal structure. Side-chain atoms, the porphyrin, and **1** were allowed to move freely during energy minimization. The resulting minimum energy complex structures were sorted by energy, and the unique structures within a 50 kJ/mol energy window above the global minimum were stored in a MacroModel multistructure file for further interactive study using the three-dimensional graphical interface of MacroModel.

Conformational analysis of the enzyme−substrate complex involved 1000 MC steps (MCMM/MOLS), and 80 unique binding conformations were stored after rejections based on the comparison of binding geometries of the substrate obtained in each step. Nonbonded atom pairs of extreme proximity give rise to very high van der Waals repulsion; therefore, trial structures having such close pairs were also discarded before minimization. Low-energy conformers were analyzed by comparing the orientation of the substrate relative to the active ferryl oxygen atom of the central heme unit. On the basis of evaluation of the distances between the ferryl oxygen atom and the closest carbon atom in each orientation of the substrate, the conformation pool could be grouped into four main families. In the largest group (family I) the C3 atom of the substrate was found to be closest to the ferryl oxygen (O*), while the remaining groups can be characterized by the shortest C6−O* (family II), C(N)−O* (family III), and C4−O* (family IV) distances, respectively. Conformational families defined above correspond to transition states leading to metabolic products. Conformations with the shortest C3−O* distance are intermediates in the formation of **2**, while conformations characterized by C(N)−O* and C6−O* contacts represent the intermediates in metabolic pathways to **3** and **4**, respectively. The metabolic product corresponding to the C4−O* contact has not yet been isolated.

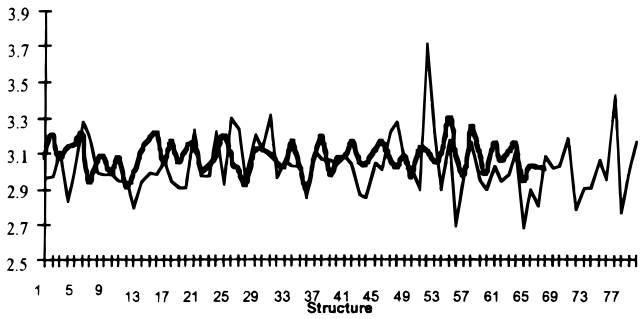

Figure 3. Distribution of the C3−O* distance during MCMM/MOLS search (light line) and MD (bold line) simulations.

These conformational search results were corroborated by a 1 fs time step, 150 ps MD simulation using the same potential energy function, nonbonded cutoff criteria, and restoring pseudopotential to restrain the site backbone atoms. The MD run was started with the same manually docked structure subjected to 2000 steps of Polaak−Ribiere conjugate gradient minimization. The crucial atomic distances used above to define conformational families were monitored after a 30 ps equilibration period. Structures were periodically sampled to save 1000 snapshots during the course of the simulation to be further subjected to energy minimization. The resulting 68 minimum energy binding conformations were compared to those found during the MCMM/MOLS conformational search, which are believed to represent all of the possible low-energy binding modes.

The 68 minimized MD structures were part of the set of 80 MCMM/MOLS structures representing all four families leading to different metabolites. Figure 3 shows the distribution of the crucial C3 carbon and ferryl oxygen (O*) distance found in the 80 MCMM/MOLS and 68 MD binding conformations, respectively. Note that the range of the C3−O* distance is larger in the MCMM/MOLS structures than it is in the MD structures. This is an indication (along with the fact that MCMM/MOLS found more binding conformations than MD) that MCMM/MOLS covered more of the conformational space of binding than MD. Indeed, on the basis of our good experience, we advocate the use of MCMM/MOLS conformational search in binding studies as an equally useful computational tool as the more popular MD simulation technique.

The global minimum energy conformation of the enzyme−substrate complex belongs to family I (E = 7538.9 kJ/mol) and is depicted in Figure 4. The central heme unit of the enzyme is colored orange, while important residues for the orientation of the substrate (red) are colored green. The C3−O* contact found in this conformation (2.698 Å) suggests the formation of the major metabolite (**2**), which is in accordance with experimental data. This orientation of **1** was found to be stabilized

(36) Fruetel, J.; Collins, J.; Camper, D. L.; Loew, G.; Ortiz de Montellano, P. R. *J. Am. Chem. Soc.* **1992,** *114*, 6987−6993.

(37) Graham-Lorence, S.; Petterson, J. A. *FASEB J.* **1996**, *10*, 206−214.

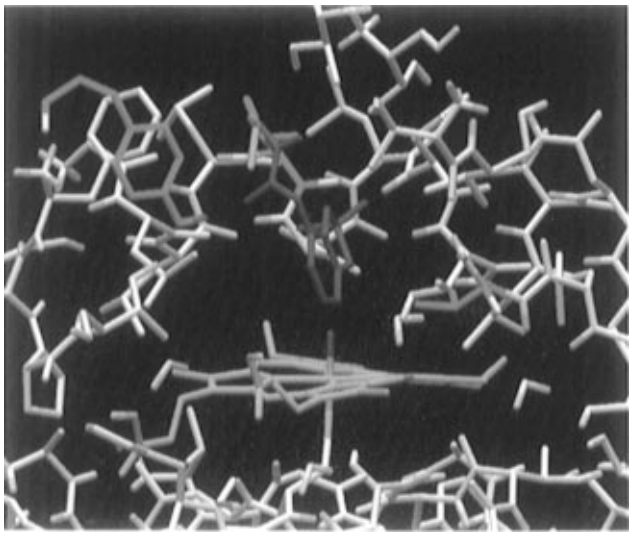

Figure 4. Global minimum of the cytochrome P-450$_{cam}$−carbofuran complex (family I) obtained by MCMM/MOLS calculations.

by a relatively strong hydrogen bond ($d_{O\cdots H}$ = 1.709 Å, $d_{O\cdots O}$ = 2.746 Å) formed between the carbamate oxygen of **1** and the aromatic hydroxy group of Tyr96. This interaction was experimentally validated by the site-specific replacement of Tyr96[38,39] and plays an important role in the orientation of the natural substrate of cytochrome P-450$_{cam}$ as well as in the binding of several camphor analogs,[40−42] styrene,[28] thioanisole,[27] and tetralone.[43] In addition to H-bonding, steric effects of Val295 and Val247 also contributed significantly to the orientation of the substrate. Methyl groups of Val295 are close to the *N*-methyl group of **1** (C−C distance 4.144 Å) while the carboxyl group of the same residue interacts with one of the methyl groups of **1** at position 2 (C−C distance 3.026 Å). The distance between the carbon atom of the methyl group of Val247 and the C3 atom of **1** was found to be 3.718 Å, suggesting that this methyl group might play a significant role in substrate orientation. H-abstraction from the C3 center leads to the corresponding radical with planar-trigonal orientation, which has two enantiotopic faces. The active oxygen of the ferryloxy unit is situated at the Si face; therefore, the configuration at the C3 atom in **2** must be *S*. This selectivity was also indicated by the fact that the steric effect of Val247 directs the *pro-S* hydrogen of C3 toward the active ferryl oxygen, i.e., it was the *pro-S* hydrogen that was found to be closer to the active oxygen than the *pro-R* hydrogen. Distances between the ferryl oxygen atom and hydrogens of C3 were found to be 1.888 and 3.693 Å for *pro-S* and *pro-R* hydrogens, respectively. As a consequence, the Si face of the radical C3 center is preferred, leading to the conclusion that only the *S* enantiomer of **2** would be formed along this metabolic path. Experimental data on the stereoselectivity of cytochrome P-450 catalyzed metabolic epoxidation have recently been reported;[44] however, no data on the hydroxylation reaction have been revealed.

(38) Attkins, W. M.; Sligar, S. G. *J. Biol. Chem.* **1988**, *263*, 18842−18849.
(39) Attkins, W. M.; Sligar, S. G. *J. Am. Chem. Soc.* **1989**, *111*, 2715−2717.
(40) White, R. E.; McCarthy, M. B.; Egeberg, K. D.; Sligar, S. G. *Arch. Biochem. Biophys.* **1984**, *228*, 493−502.
(41) Eble, K. S.; Dawson, J. H. *J. Biol. Chem.* **1984**, *259*, 14389−14393.
(42) Gelb, M. H.; Malkonen, P.; Sligar, S. G. *Biochem. Biophys. Res. Commun.* **1982**, *104*, 853−858.
(43) Gunsalus, I. C.; Wagner, G. C. In *Methods in Enzymology*; Fleischer, S., Packer, L., Eds.; Academic Press: New York, 1978; Vol. 52, Part C, p 166.
(44) Kishimoto, D.; Oku, A.; Kurihara, N. *Pestic. Biochem. Physiol.* **1995**, *51*, 12−19.

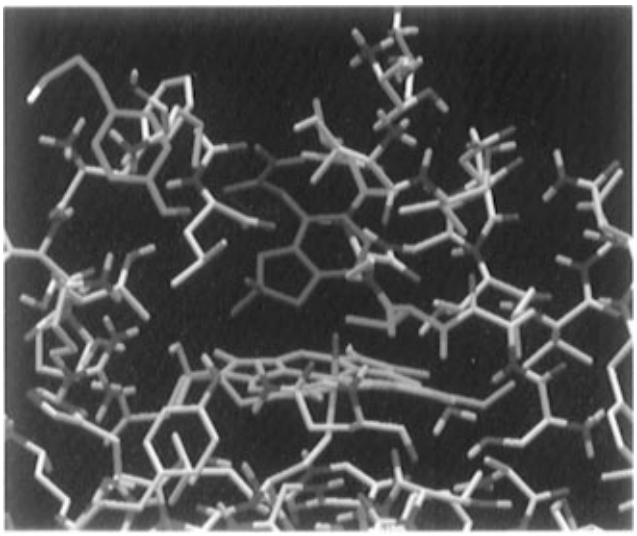

Figure 5. Lowest energy conformation of the cytochrome P-450$_{cam}$−carbofuran complex in family II obtained by MCMM/MOLS calculations.

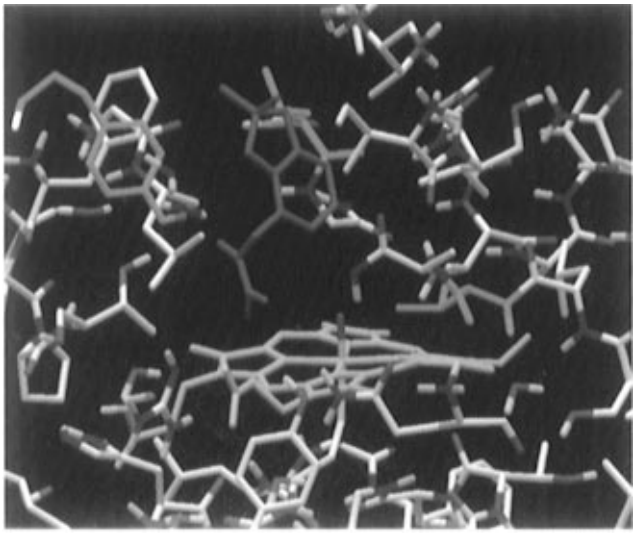

Figure 6. Lowest energy conformation of the cytochrome P-450$_{cam}$−carbofuran complex in family III obtained by MCMM/MOLS calculations.

Heats of formation of the lowest energy conformers in family II (Figure 5) and family III (Figure 6) were found to be 7551.4 and 7549.8 kJ/mol, respectively, significantly higher than that of the global minimum. The increase in energy relative to the most stable complex can be attributed to unfavorable steric effects and diminished hydrophobic interactions between the benzofuran ring of **1** and the binding site in the energetically most favored conformation of family II. The minimum energy conformation of family III shows a weak hydrogen bond to Tyr96 ($d_{O\cdots H}$ = 1.987 Å, $d_{O\cdots O}$ = 3.124 Å) which results in only a slight gain in energy in comparison to the corresponding structures in families I and II. These results can explain the experimentally observed formation of **2** in the oxidative metabolism of carbofuran.

Conclusions

The regioselective formation of 3-hydroxycarbofuran (**2**) during the oxidative metabolism of **1** was explained on the basis of calculations of the electronic properties of **1** and the enzyme−substrate interactions with cytochrome P-450$_{cam}$. We predict

that the primer metabolism of **1** should yield stereospecifically the (*S*)-3-hydroxylated metabolite **2** and small amounts of other hydroxylated products such as **3** and **4**. These predictions are in accordance with experimental data. The orientation of the substrate **1** was rationalized by systematic analysis of the geometric features in the enzyme−substrate complex. Structural information provided by our calculations can prove to be useful in the rational design of new synergists for blocking the oxidative metabolism. Selective antagonism of this metabolic system represents an alternative way to the successful management of resistance, which might lead to the application of reduced doses of pesticides.

JA9639372